Broadband Dynamics of Ubiquitin by Anionic and Cationic Nanoparticle- Assisted NMR Spin Relaxation

Stacey Wardenfelt, *[a] Xinyao Xiang, *[a] Mouzhe Xie, *[a] Lei Yu, [a] Lei Bruschweiler-Li, [b] and Rafael Brüschweiler*[a,c]

Abstract

The quantitative and comprehensive description of the internal dynamics of proteins is critical for understanding their function. Nanoparticle-assisted ¹⁵N NMR spin relaxation is a new method that uses a simple read-out allowing the observation of ps - μ s dynamics of proteins when transiently interacting with the surface of nanoparticles. The method is applied here to the widely studied protein human ubiquitin in the presence of anionic and cationic silica nanoparticles (SNP) of different size. The resulting backbone dynamics profiles are highly reproducible and strikingly similar to each other, indicating that, with the exception of the disordered tail, specific protein-SNP interactions are unimportant. The dynamics profiles closely match the sub-ns dynamics S2 values observed by model-free analysis of standard ¹⁵N relaxation of ubiquitin in free solution. These results indicate that the bulk of ubiquitin backbone dynamics in solution is confined to sub-ns timescales and, hence, it is dynamically considerably more restrained than some previous NMR studies have suggested.

Main text

Protein dynamics is an integral part of protein behavior under physiological conditions playing a critical role for many types of protein functions, such as protein-recognition and catalysis. [1],[2] NMR spectroscopy has served as a rich source of protein dynamics at atomic resolution. Much of what is known experimentally about fast nanosecond and picosecond backbone motions of proteins in solution stems from NMR transverse R_2 and longitudinal R_1 spin relaxation rates and $\{^1H\}^{-15}N$ NOEs. [3] Since these commonly used experiments are insensitive to slower timescale motions (> 5 ns), our knowledge about the presence and functional role of such slower timescale motions remains very limited. The notable gap in

knowledge about dynamics on this slower timescale regime from low ns to μs can be closed by the recently introduced nanoparticle-assisted spin relaxation method (**Figure 1**). [4] For two globular proteins (Im7 and CBD1), it revealed large-scale dynamics of functionally important loops on these slower timescales that were previously inaccessible. Here, we use this method to probe the presence of slower timescale motions in human ubiquitin. Because over the years, intramolecular dynamics of ubiquitin have been studied more thoroughly than those of most other proteins (*vide infra*), the new findings allow a detailed comparison with the rich body of previous results.

Nanoparticle-assisted spin relaxation measures transverse R_2 relaxation of a protein in the presence and absence of synthetic nanoparticles (NPs), such as silica nanoparticles (SNPs). Transient interactions between the protein and the SNPs (**Figure 1**) cause an increase in site-specific 15 N- R_2 values $^{[4]}$

$$\Delta R_{2i} = R_{2i}^{NP} - R_{2i}^{free} = c \cdot p \cdot \tau_{NP} \cdot S_i^2 \tag{1}$$

where c is a constant (see Supporting Information), p is the population of protein bound to the nanoparticle, $\tau_{\rm NP}$ is the rotational tumbling correlation time of the nanoparticle, and S_i^2 is the generalized order parameter of the N-H bond vector of residue i. In contrast to traditional model-free (MF) order parameters, S_i^2 reports on internal motions from ps to $\tau_{\rm NP}$ whereby $\tau_{\rm NP}$ can extend into the hundreds of ns to μs range depending on the nanoparticle size (**Figure 1E**). Because the presence of nanoparticles leaves R_1 unaffected (**Figure S1**), ΔR_2 is not a mere viscosity effect caused by the nanoparticles. Since chemical exchange $R_{2,\rm ex}$ affects R_2 equally in the presence and absence of SNPs, their net effect on ΔR_2 cancels out (**Figure S8**). We first describe the nanoparticle-assisted relaxation results for ubiquitin and then compare them with previous studies.

¹⁵N- R_2 relaxation rates at 850 MHz ¹H NMR frequencies were measured for uniformly ¹⁵N-labeled ubiquitin in the presence and absence of SNPs. Experiments with either anionic (pristine) or cationic (Al³⁺-doped) SNPs at 20 nm diameter (**Figure 1**) were performed at SNP concentrations in the sub-μM to low μM range. 2D ¹⁵N-¹H HSQC cross-peaks show a distinct dependence on the presence of nanoparticles in terms linewidths (R_2), whereas peak positions remain essentially unchanged (**Figure 1A-C**). These results are highly reproducible (**Figure S2**) and also fully consistent with results obtained at 600 MHz NMR field (**Figure S7**).

Department of Chemistry and Biochemistry
The Ohio State University

151 W. Woodruff Ave, Columbus, Ohio 43210, U.S.A. E-mail: bruschweiler.1@osu.edu

[b] Dr. Lei Bruschweiler-Li Campus Chemical Instrument Center The Ohio State University 151 W. Woodruff Ave, Columbus, Ohio 43210, U.S.A.

Prof. Rafael Brüschweiler,
 Department of Biological Chemistry and Pharmacology
 The Ohio State University, Columbus, Ohio 43210, U.S.A.

+ Stacey Wardenfelt, Xinyao Xiang and Mouzhe Xie are co-first authors.

Supporting information for this article is given via a link at the end of the document.

[[]a] Stacey Wardenfelt, Xinyao Xiang, Mouzhe Xie, Lei Yu, Prof. Rafael Brüschweiler

S² profiles for both anionic and cationic nanoparticles derived from $^{15}\text{N-}\Delta R_2$ values are depicted in Figure 2A. Because the stability of colloidal SNP dispersions varies with nanoparticle type and pH, measurements with anionic and cationic SNPs were conducted at pH 6 and pH 5, respectively. Because the prefactor $c \cdot p \cdot au_{_{NP}}$ in Eq. (1) is only approximately known, ΔR_2 were converted to S² values via global scaling to mean standard model-free order parameters S^2_{MF} obtained for nanoparticle-free ubiquitin. Both ΔR_2 -derived dynamics profiles show rigid secondary structures (high S2), which include the α -helix and β -strands, and regions with increased mobility (low S²), namely the loop of the N-terminal β-hairpin and five residues in the C-terminal tail. Both anionic and cationic ΔR_2 profiles show remarkably similar profiles consistent with predominantly nonspecific interactions between ubiquitin and the nanoparticles. These findings are supported by structure-based computational identification of the most and least preferred contact sites between ubiquitin and anionic and cationic SNPs, which reveals a sizeable number of such sites (Figure 3) that broadly correlate with the electrostatic surface potential of ubiquitin (Figure S5).

Close inspection of the mobile regions reveals slightly reduced S² values for cationic vs. anionic SNPs. The β-hairpin loop with sequence L8-T9-G10-K11-T12 can display electrostatic attraction with the N_EH₃⁺ amino group of K11 to anionic SNPs and repulsion with respect to cationic SNPs, whereby the attractive interaction causes very slight rigidification of this loop. Similarly, the C-terminal tail with sequence L71-R72-L73-R74-G75-G76, known to be intrinsically disordered, contains two basic residues R72 and R74 that are attracted to anionic SNPs by Coulomb forces. Although the corresponding S2 values are somewhat elevated, the tail remains disordered (Figure 2A). This behavior is consistent with recent NMR relaxation studies of the interactions of intrinsically disordered proteins with anionic SNPs and affirms electrostatic interactions as a major driving force. [5] This also suggests that transient interactions between ubiquitin and the nanoparticles do not significantly rigidify the protein.

To compare the nanoparticle-assisted relaxation results with standard model-free analysis, ^[6] backbone S^2_{MF} order parameters were determined from R_1 , R_2 , and $\{^1H\}^{-15}N$ NOEs at pH 6 in the absence of SNPs (black symbols in **Figure 2A**). Both nanoparticle-assisted S^2 profiles agree remarkably well with the S^2_{MF} results. They even display the same fine zig-zag patterns, which include residue clusters 2-6, 15-17, 34-36, 48-50, 61-63, 65-70. As expected for anionic SNPs, the largest deviation is found in the flexible C-terminus where $S^2 > S^2_{MF}$.

According to Eq. (1), S^2 reflects the presence of motions with correlation times τ_{int} from ps all the way to τ_{NP} , which covers 9 decades of timescales. For spherically shaped nanoparticles of radius r (**Figure 1D**), τ_{NP} follows the Stokes-Einstein-Debye relationship

$$\tau_{\rm int} < \tau_{NP} = \frac{4\pi r^3 \eta}{3k_{\scriptscriptstyle B} T} \tag{2}$$

where η is the water solvent viscosity, $k_{\rm B}$ is the Boltzmann constant and T is the absolute temperature. Hence, a systematic change of nanoparticle size permits control of the timescale window to which ΔR_2 is sensitive to (Figure 1E). We used 3 differently sized anionic nanoparticles with average diameters of 9, 20, and 45 nm (Figure **S6**), which according to Eq. (2) have at 298 K average τ_{NP} around 83 ns, 0.91 μ s, and 10 μ s, respectively. Interestingly, the resulting S² profiles, which are depicted in Figure 2B, show very little change as a function of nanoparticle size. This suggests that shifting of the nanoparticle rotational tumbling rate neither obscures nor reveals additional internal dynamics of ubiquitin. Together with the observed excellent agreement between S2MF and S2, our results show that on the ps $-\mu s$ window accessed here, the dominant internal backbone motions occur on the ps to low ns timescale. The data do not provide evidence for the existence of slower timescale backbone motions that extend into the tens of nanosecond to low us range.

The backbone dynamics of ubiquitin in solution has been the subject of numerous quantitative NMR investigations. However, no clear consensus has been reached about the existence and the details of slower timescale motions. Several ^{15}N -relaxation studies at high magnetic field were reported $^{[7],[8],[9],[10],[11]}$ with MF order parameters S^2_{MF} and internal correlation times in the sub-ns, which were highly consistent with each other and also with the S^2_{MF} reported here. A ^{15}N -relaxometry study performed with B_0 -fields from $0.5-22.3~\text{T}^{[12]}$ reported several regions with enhanced mobility (S^2_{RO} < 0.7) with correlation times up to 5 ns, even for regions that are notably rigid on the sub-ns timescale (S^2_{MF} > 0.80) (**Figure 2C**). Such regions include the β -hairpin loop (residues 7-12), the β_2 -strand (residues 13-17), and the long stretch of residues 46-55. Such augmented levels of dynamics lie outside of the experimental error bars of any of these measurements (**Figure S4B**).

Residual 15N-1H dipolar couplings (RDCs) are potentially affected by an even broader range of motional timescales from ps to sub-ms. However, disambiguation of the effects of structure and dynamics is notably challenging as it requires measurements in ≥5 different alignment media. The DIDC method[13],[14] with RDC data from 6 alignment media led to a S²_{RDC} profile (Figure 2C) that overall resembles the S²_{MF} and nanoparticle-assisted S² profiles, except that the S²_{RDC} profile was systematically shifted toward significantly lower values. An extensive RDC data set measured for 23 - 36 different alignment media also produced a S2RDC profile with many low order parameters (Figure 2C).[15] Common to the RDC methods is that they provide only relative S2 values. The S2RDC profile is globally scaled so that none of the RDC-derived S2RDC exceeds any of the $S^2_{\ MF}$ values. This makes the final profiles prone to systematic offsets caused by experimental errors of S²_{RDC} at few sites. Ubiquitin is also potentially malleable by the presence of some alignment media

causing heterogeneous structural behavior across the different media, which can be hard to disambiguate from noisy data. [13],[16],[17]

As an alternative to model-free RDC approaches, explicit molecular ensembles were constructed that depict the structural heterogeneity of ubiquitin encoded in the RDC data. These ensembles were built with different sizes with the help of additional NMR constraints $(NOEs)^{[18],[19]}$ or accelerated molecular dynamics simulations. When using the same RDCs as input, they generally produce dynamics profiles similar to the S^2_{RDC} profiles, although minimalistic ensembles can also produce a satisfactory explanation of the raw data while being dynamically significantly more restrained. In addition to the many NMR studies in solution, ubiquitin dynamics was investigated also in the solid state by spin relaxation and dipolar couplings. Paper also produce S^2_{solid} parameters are notably similar to the nanoparticle-assisted S^2 results reported here (Figure S4).

Nanoparticle-assisted relaxation offers a re-examination of the internal dynamics of ubiquitin, a thermodynamically unusually stable human protein with an unfolding temperature above 100 °C.[25] Although ubiquitin is one of the best studied proteins by NMR, important questions about its backbone dynamics are still open. This new method permits a highly quantitative and reproducible broadband view of protein dynamics sensitive to ps to us timescales. Our results are largely indifferent to the net charge of the nanoparticles suggesting that specific protein-NP interactions do not significantly affect dynamics with the exception of the highly flexible tail. Besides the tail, the results depict ubiquitin as a mostly rigid protein along its backbone, a behavior that is pervasive across the broad spectrum of timescales probed here. The loop region of the Nterminal β-hairpin 7-13 shows only modest amounts of increased dynamics, very similar as those seen by standard MF analysis of free protein. Our data also do not show a dependence on nanoparticle size suggesting that no additional detectable internal backbone dynamics takes place on the 100 ns to low µs timescale. While bound to the SNP surface, ubiquitin could undergo restricted global tethering motions. If present, such effects are expected to be anisotropic and different for anionic vs. cationic SNPs and, hence, they would result in differential mean S2 values among secondary structures in an SNP-type dependent manner. The absence of any such behavior of the experimental S2 profiles (Figure 2A) suggests that tethering effects are not significant.

The nanoparticle-assisted relaxation approach is sensitive to internal motions on sub- τ_{NP} timescales (**Figure 1E**) provided that the exchange rate k_{ex} of the protein with the nanoparticle is not too fast. If $k_{ex} \geq 1/\tau_{P}$, ΔR_2 tends toward zero and if $k_{ex} \geq 1/\tau_{int}$, the apparent S^2 values approaches 1. Based on the proteins studied by this approach so far,^[4] we expect that τ_{NP} is presently the limiting factor for the observation of slow internal motions. Ubiquitin is known to undergo additional backbone dynamics involving the N-terminus of the α -helix and a flip of peptide bond D52-G53 accompanied by a

subtle contraction and expansion. The former is visible as $R_{2,\text{ex}}$ in the both R_2 profiles in the presence and absence of nanoparticles (**Figure S8**), but it cancels out in ΔR_2 as it occurs on a timescale slower than those accessible here (> 10 μ s). ^[26] By developing suitably large nanoparticle systems, it may be possible to bridge the gap between nanoparticle-assisted dynamics and conformational exchange dynamics studied by CPMG-type experiments.

Together, these results demonstrate that the loop samples its major conformational substates on the sub-ns range, consistent with S^2_{MF} results, and the absence of significant slow time-scale dynamics in the ns – μs range. These results are similar to a recent solid-state NMR study, $^{[23]}$ but are at variance with other studies mentioned above (**Figure 2C**), including RDC-based dynamics studies, that inferred large amplitude motions on timescales comparable to or slower than the tumbling correlation time of free protein. Although the RDC studies were conducted with great care, RDC data fitting for dynamics analysis is exquisitely sensitive to noise and the many different experimental alignment conditions.

The new nanoparticle-assisted relaxation approach is notably robust because (i) it is only sensitive to dynamics, but not to structure, (ii) in its simplest form it requires ¹⁵N-R₂-relaxation measurements of only two samples, one in the presence and one in the absence of nanoparticles, and (iii) the read-out of S² is straightforward without the need of non-linear least squares fitting of model parameters. This makes this method a versatile tool to comprehensively study internal dynamics of biomolecules in solution. Its application should provide clear evidence about both the presence and absence of slower internal dynamics in biomolecules in solution and their possible functional roles that are beyond the reach of current methods.

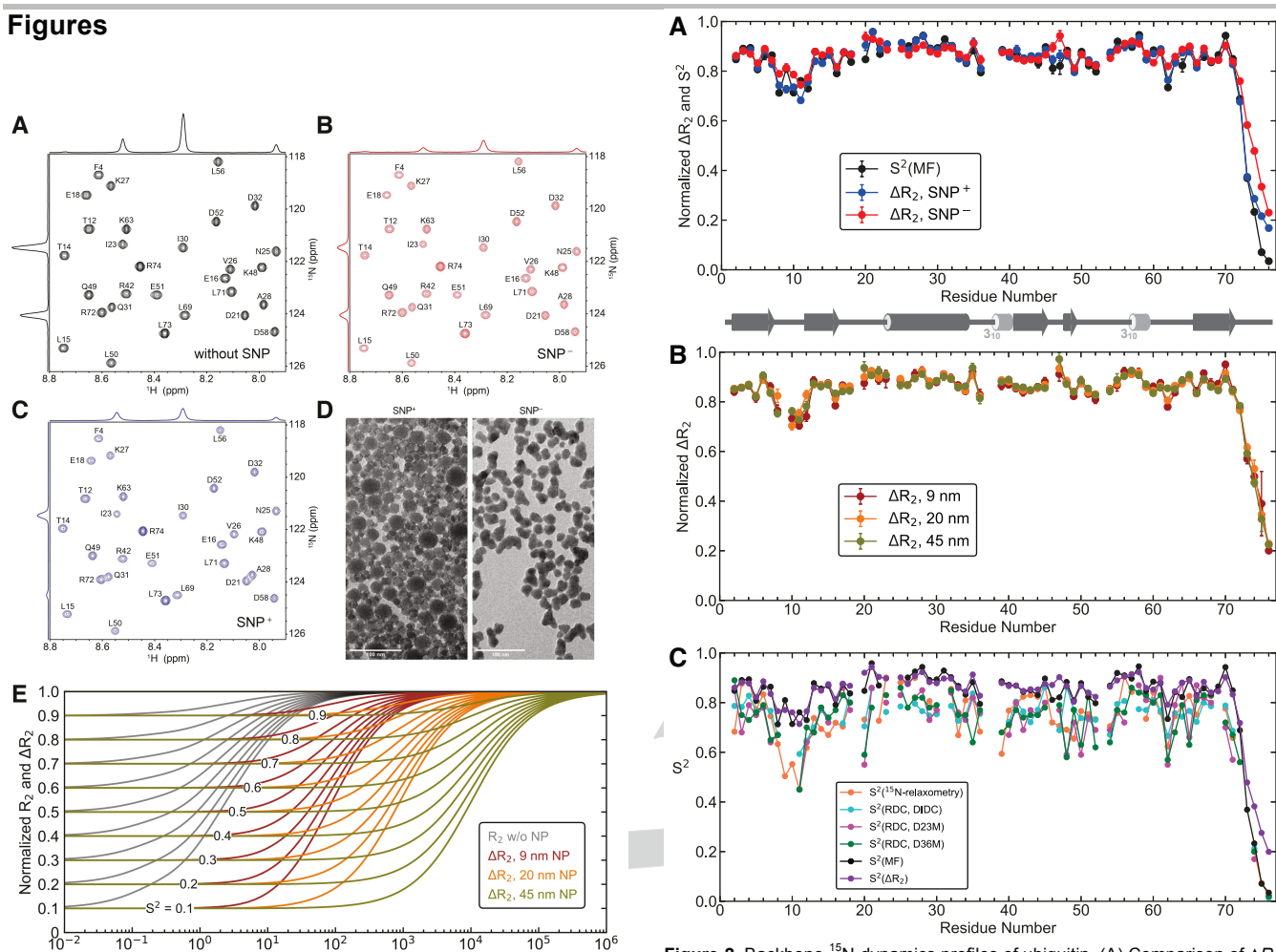


Figure 1. ¹⁵N-¹H HSQC spectra of ubiquitin with and without anionic or cationic SNPs (SNP and SNP), TEM nanoparticle images, and simulated dependence of ΔR_2 on internal motional protein timescales. Region of $^{15}N-^1H$ HSQC with 1D cross-sections at the position of resonance I30 (A) in the absence of SNP at pH 6, (B) in the presence of SNP at pH 6, and (C) in the presence of $\mathsf{SNP}^{^+}$ at pH 5. The reduction in cross-peak intensities reflects peak broadening and loss of magnetization through accelerated relaxation in the presence of SNPs. (D) TEM images are shown of 20 nm SNP+ (left) and 20 nm SNP (right). (E) Simulated dependence of transverse R2 relaxation rates in the absence of NPs and ΔR_2 (increase in R_2 upon the addition of NPs) on the internal correlation time τ_{int} and order parameter $S^2.$ The rotational tumbling correlation time of the globular protein τ_{P} was set to 4.0 ns and the τ_{NP} of NPs were calculated from Eq. (2) (83 ns, 0.91 $\mu s,$ and 10 μs for 9 nm, 20 nm, and 45 nm diameter NPs, respectively). R_2 and ΔR_2 were uniformly scaled so that their maximal values are 1.0. ΔR_2 probes internal motions on a wide range of timescales from ps to μs , depending on the size of NPs and protein, exceeding the observable timescale window of classical spin relaxation by 100- to 10,000-fold.

τ_{int} (ns)

Figure 2. Backbone ¹⁵N-dynamics profiles of ubiquitin. (A) Comparison of ΔR_2 -derived S² for 20 nm SNP* (blue, pH 5) and 20 nm SNP* (red, pH6) with standard model-free order parameters S²_{MF} (black, pH 6). Ubiquitin dynamics on ps-ns timescales is essentially unaffected over the pH range 4 – 7 (Figure S3). The secondary structure of ubiquitin is indicated at the bottom with β-strands as arrows and helices as cylinders. (B) ΔR_2 -derived S² using 9, 20, and 45 nm anionic SNPs. T9 and A46 are excluded due to weak signals caused by hydrogen exchange with H₂O at pH 7. (C) Comparison of ΔR_2 -derived S² (average over the SNP* and SNP* results in (A)) and S²_{MF} with previous studies in solution, including ¹⁵N-relaxometry, ^[12] RDC DIDC method using 6 alignment media, ^[13] and SCRM analysis using 23 or 36 alignment media (labelled as D23M and D36M). ^[15] The same plot with error bars is depicted in Supporting Information (Figure S4B). All ΔR_2 profiles were converted to S² profiles by global scaling with respect to S²_{MF} based on the regions with rigid secondary structures (high S²_{MF} values).

[19]

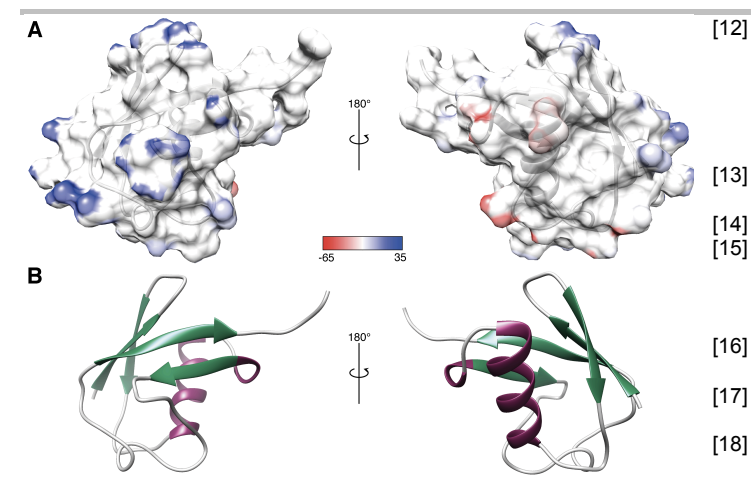


Figure 3. Predicted sites with most and least preferential interactions between ubiquitin with nanoparticle surface. (A) Space filling model of ubiquitin with its surface atoms colored in blue (red) that are in direct contact with SNP surface and have strongest (weakest) attractive interaction with SNP (SNP) (see Supporting Information for details). (B) Ribbon model of ubiquitin with colored secondary structures depicting same 3D structure and same orientations as in (A).

Acknowledgements

We thank Drs. Alexandar L. Hansen and Da-Wei Li for helpful discussion; Drs. Joel Tolman and Fabien Ferrage provided their published data for Figure 2C. Nouryon provided all nanoparticles used in this work as a gift. This work was supported by the National Science Foundation (MCB-1360966). All NMR experiments were performed at the CCIC NMR facility at OSU.

Keywords: Protein dynamics • NMR spectroscopy • Ubiquitin • Nanoparticle-assisted NMR

References

- [1] M. Karplus, J. Kuriyan, Proc. Natl. Acad. Sci. U. S. A. 2005. 102, 6679-6685.
- [2] M. Kovermann, P. Rogne, M. Wolf-Watz, Q. Rev. Biophys. 2016, 49, 43.
- [3] J. Cavanagh, W. J. Fairbrother, A. G. Palmer, M. Rance, N. J. Skelton, Protein NMR Spectroscopy: Principles and Practice, 2nd Edition 2007, 1-888.
- [4] M. Xie, L. Yu, L. Brüschweiler-Li, X. Xiang, A. L. Hansen, R. Brüschweiler, Sci. Adv. 2019, 5, eaax5560.
- M. Xie, D. W. Li, J. Yuan, A. L. Hansen, R. Brüschweiler, *Chem.-Eur. J.* 2018, 24, 16997-17001. M. Xie, A. L. Hansen, J. Yuan, R. Brüschweiler, *J. Phys. Chem. C* 2016, 120, 24463. D. W. Li, M. Xie, R. Brüschweiler, *J. Am. Chem. Soc.* 2020, 142, 24, 10730-10738.
- [6] G. Lipari, A. Szabo, J. Am. Chem. Soc. 1982, 104, 4546-4559.
- [7] D. M. Schneider, M. J. Dellwo, A. J. Wand, *Biochemistry* 1992, 31, 3645-3652.
- [8] N. Tjandra, S. E. Feller, R. W. Pastor, A. Bax, J. Am. Chem. Soc. 1995, 117, 12562-12566.
- [9] S. F. Lienin, T. Bremi, B. Brutscher, R. Brüschweiler, R. R. Ernst, J. Am. Chem. Soc. 1998, 120, 9870-9879.
- [10] S. L. Chang, N. Tjandra, J. Magn. Reson. 2005, 174, 43-53.
- [11] C. A. Castaneda, A. Chaturvedi, C. M. Camara, J. E. Curtis, S. Krueger, D. Fushman, *Phys. Chem. Chem. Phys.* 2016, 18, 5771-5788.

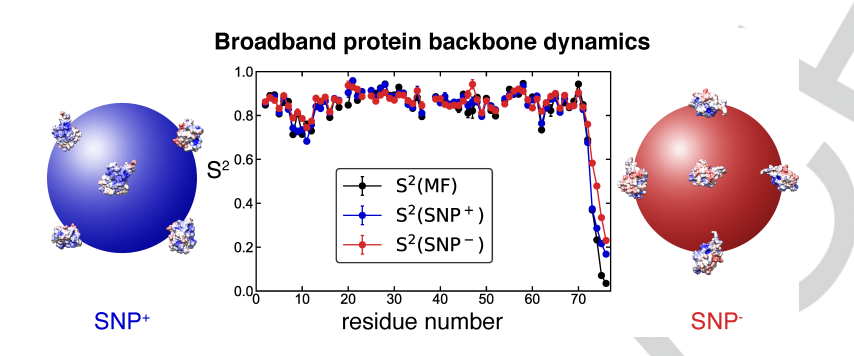
C. Charlier, S. N. Khan, T. Marquardsen, P. Pelupessy, V. Reiss, D. Sakellariou, G. Bodenhausen, F. Engelke, F. Ferrage, *J. Am. Chem. Soc.* **2013**, *135*, 18665-18672. N. Bolik-Coulon, P. Kaderavek, P. Pelupessy, J.-N. Dumez, F. Ferrage, S. F. Cousin, *J. Magn. Reson.* **2020**, *313*, 106718.

- K. B. Briggman, J. R. Tolman, *J. Am. Chem. Soc.* **2003**, *125*, 10164-10165.
- J. R. Tolman, K. Ruan, *Chem. Rev.* **2006**, *106*, 1720-1736. N. A. Lakomek, K. F. A. Walter, C. Fares, O. F. Lange, B. L. de Groot, H. Grubmuller, R. Brüschweiler, A. Munk, S. Becker, J. Meiler, C. Griesinger, *J. Biomol. NMR* **2008**, *41*, 139-155.
- J. C. Hus, R. Brüschweiler, *J. Biomol. NMR* **2002**, *24*, 123-132.
- J. C. Hus, W. Peti, C. Griesinger, R. Brüschweiler, *J. Am. Chem. Soc.* **2003**, *125*, 5596-5597.
- O. F. Lange, N. A. Lakomek, C. Fares, G. F. Schroder, K. F. A. Walter, S. Becker, J. Meiler, H. Grubmuller, C. Griesinger, B. L. de Groot, *Science* **2008**, *320*, 1471-1475. R. B. Fenwick, S. Esteban-Martin, B. Richter, D. Lee, K. F. A. Walter, D. Milovanovic, S. Becker, N. A. Lakomek, C. Griesinger, X. Salvatella, *J. Am. Chem. Soc.* **2011**, *133*, 10336-10339.
- [20] L. Salmon, G. Bouvignies, P. Markwick, N. Lakomek, S. Showalter, D. W. Li, K. Walter, C. Griesinger, R. Brüschweiler, M. Blackledge, *Angew. Chem.-Int. Edit.* 2009, 48, 4154-4157.
- [21] L. Salmon, G. Bouvignies, P. Markwick, M. Blackledge, Biochemistry 2011, 50, 2735-2747.
- [22] G. M. Clore, C. D. Schwieters, J. Am. Chem. Soc. 2004, 126, 2923-2938.
- [23] J. D. Haller, P. Schanda, J. Biomol. NMR 2013, 57, 263-280.
- [24] N. A. Lakomek, S. Penzel, A. Lends, R. Cadalbert, M. Ernst, B. H. Meier, *Chem. Eur. J.* 2017, 23, 9425-9433.
 [25] G. I. Makhatadze, M. M. Lopez, J. M. Richardson, S. T. Thomas, *Protein Sci.* 1998, 7, 689-697.
- [26] C. A. Smith, D. Ban, S. Pratihar, K. Giller, M. Paulat, S. Becker, C. Griesinger, D. Lee, B. L. de Groot, *Proc. Natl. Acad. Sci. U. S. A.* 2016, 113, 3269-3274.

Entry for the Table of Contents

COMMUNICATION

Nanoparticleassisted NMR relaxation applied to ubiquitin reveals a remarkable indifference of protein dynamics to nanoparticle charge and size indicating the absence of significant amounts of slow timescale dynamics from ps – low µs.



Stacey Wardenfelt, Xinyao Xiang, Mouzhe Xie, Lei Yu, Lei Brüschweiler-Li, and Rafael Brüschweiler*

Page No. – Page No.
Broadband
Dynamics of
Proteins by Anionic
and Cationic
NanoparticleAssisted NMR Spin
Relaxation

Author ORCID information

Name: Stacey Wardenfelt ORCID: 0000-0002-7055-2164

Name: Xinyao Xiang

ORCID: 0000-0002-8584-3642

Name: Mouzhe Xie

ORCID: 0000-0002-2960-644X

Name: Lei Yu

ORCID: 0000-0003-0159-1968

Name: Lei Bruschweiler-Li ORCID: 0000-0002-2409-7068

Name: Rafael Brüschweiler ORCID: 0000-0003-3649-4543